doi:10.1093/brain/awq067 Brain 2010: 133; 1428–1437 | 1428

BRAIN
A JOURNAL OF NEUROLOGY

Localized cerebral energy failure in DNA polymerase gamma-associated encephalopathy syndromes

Charalampos Tzoulis,[1,2] Gesche Neckelmann,[3] Sverre J. Mørk,[4] Bernt E. Engelsen, Carlo Viscomi,[5] Gunnar Moen,[3] Lars Ersland,[6,7] Massimo Zeviani[5] and Laurence A. Bindoff[1,2]

1 Department of Neurology, Haukeland University Hospital, Bergen 5021, Norway
2 Department of Clinical Medicine, University of Bergen, Bergen 5021, Norway
3 Department of Radiology, Haukeland University Hospital, Bergen 5021, Norway
4 Department of Pathology, Haukeland University Hospital, Bergen 5021, Norway
5 Unit of Molecular Neurogenetics, Pierfranco and Luisa Mariani Centre for the Study of Children's Mitochondrial Disorders, National Neurological Institute 'C. Besta', via Temolo 4, 20133 Milan, Italy
6 Department of Clinical Engineering, Haukeland University Hospital, Bergen 5021, Norway
7 Department of Surgical Sciences, Haukeland University Hospital, Bergen 5021, Norway

Correspondence to: Prof. Laurence Bindoff,
Department of Neurology, Haukeland University Hospital,
5021 Bergen, Norway
E-mail: laurence.bindoff@nevro.uib.no

Mutations in the catalytic subunit of the mitochondrial DNA-polymerase gamma cause a wide spectrum of clinical disease ranging from infantile hepato-encephalopathy to juvenile/adult-onset spinocerebellar ataxia and late onset progressive external ophthalmoplegia. Several of these syndromes are associated with an encephalopathy that characteristically shows episodes of rapid neurological deterioration and the development of acute cerebral lesions. The purpose of this study was to investigate the nature, distribution and natural evolution of central nervous system lesions in polymerase gamma associated encephalopathy focusing particularly on lesions identified by magnetic resonance imaging. We compared radiological, electrophysiological and pathological findings where available to study potential mechanisms underlying the episodes of exacerbation and acute cerebral lesions. We studied a total of 112 magnetic resonance tomographies and 11 computed tomographies in 32 patients with polymerase gamma-encephalopathy, including multiple serial examinations performed during both the chronic and acute phases of the disease and, in several cases, magnetic resonance spectroscopy and serial diffusion weighted studies. Data from imaging, electroencephalography and post-mortem examination were compared in order to study the underlying disease process. Our findings show that magnetic resonance imaging in polymerase gamma-related encephalopathies has high sensitivity and can identify patterns that are specific for individual syndromes. One form of chronic polymerase gamma-encephalopathy, that is associated with the *c.1399G>A* and *c.2243G>C* mutations, is characterized by progressive cerebral and cerebellar atrophy and focal lesions of the thalamus, deep cerebellar structures and medulla oblongata. Acute encephalopathies, both infantile and later onset, show similar pictures with cortical stroke-like lesions occurring during episodes of exacerbation. These lesions can occur both with and without electroencephalographic evidence of concurrent epileptic activity, and have diffusion, spectroscopic and histological profiles strongly suggestive of neuronal energy failure. We suggest therefore that both infantile and later onset polymerase gamma related encephalopathies are part of a continuum.

Keywords: polymerase gamma; magnetic resonance imaging; pathology; diffusion; Alpers' syndrome

Received December 9, 2009. Revised February 1, 2010. Accepted February 22, 2010. Advance Access publication April 16, 2010

Abbreviations: HLA = human leucocyte antigen; MELAS = mitochondrial encephalomyopathy lactic acidosis and stroke-like episodes; MSCAE = mitochondrial spinocerebellar ataxia and epilepsy; POLG = polymerase gamma

Introduction

Encephalopathy syndromes associated with mutations of the mitochondrial DNA-polymerase gamma (POLG) occur in differing clinical settings ranging from infantile-onset Alpers' syndrome, to adult-onset mitochondrial spinocerebellar ataxia and epilepsy (MSCAE), also known as mitochondrial recessive ataxic syndrome (Ferrari *et al*., 2005; Hakonen *et al*., 2005; Tzoulis *et al*., 2006; Engelsen *et al*., 2008). While the genotype, age of onset, severity and clinical picture may vary, POLG-encephalopathies have several common features including selective involvement of the nervous system and liver and the occurrence of episodes of exacerbation comprising rapidly progressive disturbance of consciousness, severe epilepsy and the development of acute cerebral lesions with a predilection for the posterior parts of the brain.

The pathogenesis of POLG-related disease involves secondary damage of mitochondrial DNA in the form of tissue-specific multiple deletions and/or quantitative depletion (Del Bo *et al*., 2003; Ferrari *et al*., 2005; Winterthun *et al*., 2005). Damage to mitochondrial DNA would be expected to affect aerobic respiration and lead to ATP depletion. While a variety of studies have shown respiratory chain defects, including complex I deficiency in post-mortem brain (Hakonen *et al*., 2008), or complex I, III and IV defects in muscle and liver biopsies (Nguyen *et al*., 2005; de Vries *et al*., 2007; Sarzi *et al*., 2007), the findings are inconsistent (Winterthun *et al*., 2005). Moreover, the question of whether *in vivo* energy failure occurs in the most affected tissue, namely brain, does not appear to have been addressed in detail.

In order to study the question of pathogenesis in more detail, we investigated the nature, distribution and evolution of the lesions in POLG associated encephalopathy using magnetic resonance imaging modalities. Our findings suggest that energy failure is a major element in the evolution of the encephalopathy.

Materials and methods

We studied 32 patients, 28 of which had MSCAE caused by the c.*1399G>A* (p.A467T) and/or c.*2243G>C* (p.W748S), and 4 had Alpers' syndrome; some of the clinical features of 22 of these have been described (Tzoulis *et al*., 2006; Engelsen *et al*., 2008).

Radiological investigations

A total of 112 MRI and 11 CT examinations were studied. In 25 patients (21 MSCAE and 4 Alpers'), sequential examinations were available, allowing us to study lesion evolution both during the chronic and acute phases of the disease. Diffusion imaging was performed in 10 patients (7 MSCAE and 3 Alpers') and apparent diffusion coefficient values were measured in 17 lesions.

MRI was performed on a Siemens Magnetom Symphony 1.5T scanner with 30 mT/m gradients or a General Electric Signa Excite 3T HDX scanner with 40 mT/m gradients. Sequences included T1 (unenhanced and gadolinium enhanced), T_2 and T_2 fluid-attenuated inversion recovery. Diffusion imaging was performed with *b* values of 0, 500 and 1000. Apparent diffusion coefficient measurements on selected regions of interest were performed using the software package nordicICE (NordicImagingLab, Bergen, Norway, www.nordicimaginglab.com). All apparent diffusion coefficient values are given in $\times 10^{-3}$ mm^2/s. Magnetic resonance angiography was performed on three patients and conventional cerebral angiography on one. Proton single voxel magnetic resonance spectroscopy was performed in three patients using an eight-channel head coil, the PRESS sequence (repetition time/echo time 1500/144 and 35 ms, acquisition time 3 min 48 s) and a voxel size of 8 ml. In Patient AT-1B, spectra were recorded from a fresh, right occipital lesion and the unaffected contralateral occipital area, 70 days after clinical onset of the exacerbation episode. In Patient WS-1A measurements were done in a fresh right parietal lesion, 28 days after onset. In Patient AT-1A, no new lesions were seen and measurements were made from an apparently normal right frontal lobe and an old cerebellar white matter lesion.

Genetic investigations

Genomic DNA was isolated from blood using standard protocols and *POLG* exons 2–23 were amplified using standard procedures and AmpliTaq Gold DNA polymerase (ABI, Foster city, USA), including at least 50 bases of flanking intronic sequence. Sequencing was performed using BigDye Terminator cycle sequencing kit (v1.1, Applied Biosystems). Reference sequence for the *POLG*-gene: NM_002693.1. Nomenclature used is according to international recommendations (http://www.hgvs.org/rec.html).

Pathology

Post-mortem examination was performed in seven patients (AT-1A, AT-1B, AT-2A, WS-1A, WS-2A, WS-12A and AL-1B) with detailed pathological investigations of the brain, spinal cord and liver performed in three (AT-1A, AT-1B and WS-1A). Haematoxylin-eosin and luxol fast blue staining were performed using standard procedures. Immunohistochemical investigations were performed using antibodies directed against glial fibrillary acidic protein, human leucocyte antigen (HLA)-DR/DP/DQ a microglial marker, and CD68, a monocyte marker. Antibodies were obtained from DAKO, Glostrup, Denmark. Double staining for cytochrome oxidase and succinate dehydrogenase was performed in frozen brain sections of Patients AT-1A (left and right occipital, right frontal, right cerebellum) and AL-1B (left occipital, left frontal, right cerebellum) as described previously (Betts *et al*., 2006).

Results

Genetics

The MSCAE patients were either homozygous for the c.*1399G>A* (p.A467T), or homozygous for the c.*2243G>C* (p.W748S), or compound heterozygous in *trans* for these two mutations

(p.A467T/W748S). Patient AL-2A had the A467T and c.2542G>A (p.G848S) on different alleles. Two brothers AL-1A and AL-1B, and another unrelated child AL-3A carried the A467T in *trans* with the novel c.907G>A in exon 4, which replaces a highly conserved glycine residue with an arginine at position 303 (G303R) in the exonuclease region of *POLG*. The G303R was not found in >170 other patients and controls in whom we have sequenced the entire *POLG* coding region.

Classification and evolution of neuroradiological findings

Imaging findings fell into three categories: acute stroke-like lesions, chronic focal signal abnormalities and slowly progressive atrophy (Figs 1 and 2, Table 1). Acute stroke-like lesions and chronic focal lesions exhibited consistently high T_2 and low T_1 signal. The most sensitive MRI sequences for detecting signal changes were fluid-attenuated inversion recovery-T_2 and diffusion weighted imaging. All three types of changes were seen in MSCAE, while only stroke-like lesions occurred in the Alpers' cases.

Stroke-like lesions occurred in 23 out of 32 patients (19 out of 28 MSCAE and all four Alpers'). They appeared exclusively during episodic exacerbations when the patient presented with focal and generalized epileptic seizures and rapidly progressive encephalopathy. Stroke-like lesions affected, in order of decreasing frequency, the occipital (19 out of 23), parietal (12 out of 23), frontal (11 out of 23), lateral temporal (5 out of 23) and cerebellar (4 out of 23) cortices, while the medial temporal lobes and hippocampi were universally spared. The central pons was affected in one case (AT-1A). Stroke-like lesions evolved dynamically during the course of the episodes, mirroring clinical severity and progression of the encephalopathic symptoms. Persistence or progressive worsening of the encephalopathy was associated with gradual lesion expansion and/or the appearance of new lesions (Fig. 2A and B). Epileptic activity was not a prerequisite for the progression of the stroke-like lesions, which often expanded inexorably also after the seizures had been successfully controlled clinically and on EEG.

EEG was performed during exacerbation episodes in 17 patients with acute stroke-like lesions. Twelve of these had focal epileptic activity that correlated to one or more stroke-like lesion localizations. One had generalized epileptic activity, while the remaining four had focal epileptic activity that did not correlate with the location of any of their lesions. Nine patients had early EEG, performed 0–4 days from episode onset. Four of these had initially no epileptic activity, but generalized slow-wave activity that in three out of four was maximal over the stroke-like lesions area. Epileptic activity developed in these foci on later recordings.

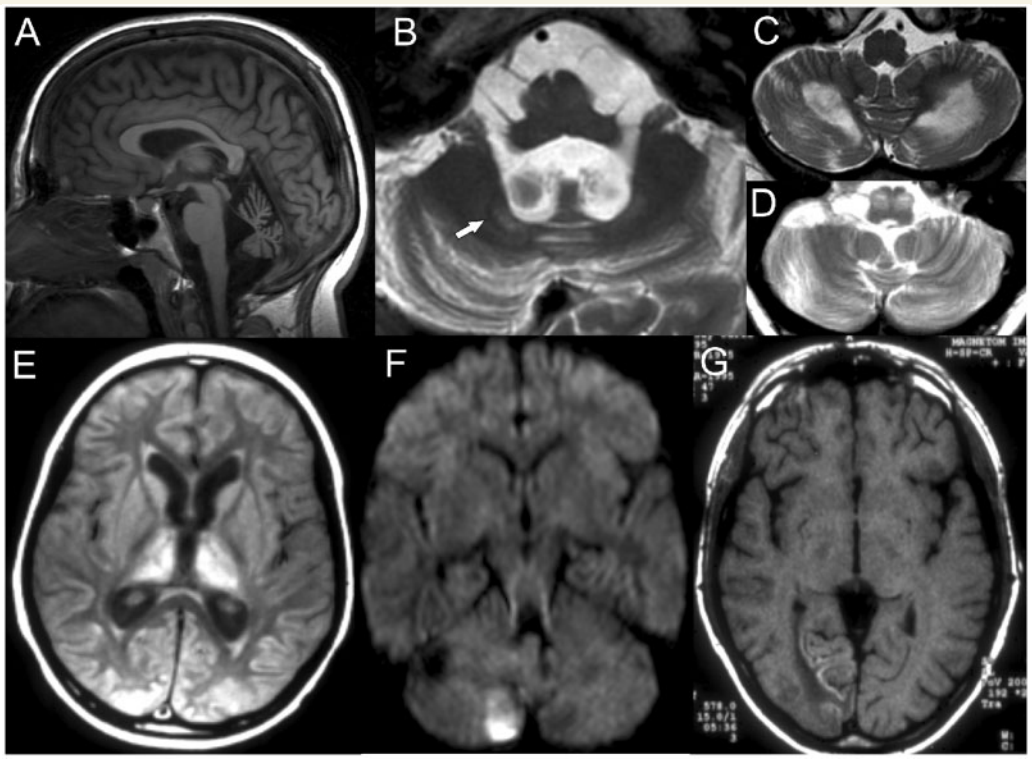

Figure 1 MRI findings in POLG-encephalopathy. (**A**) Sagittal T_1 image showing cerebellar atrophy in Patient WS-10A. (**B**) Axial T_2 image showing dentate atrophy (arrow) in Patient WS-10A. (**C**) Axial T_2 image showing cerebellar white matter hyperintensity in Patient AT-1A. (**D**) Axial T_2 image showing bilateral olivary lesions in Patient WS-4A. The olives appear enlarged and hyperintense. (**E**) Axial T_2 fluid-attenuated inversion recovery image showing bilateral thalamic and cortical occipital lesions in Patient WS-9A. (**F**) Axial diffusion weighted image ($b = 1000$) showing an acute stroke-like lesions in the right cerebellar cortex of Patient AL-1A. (**G**) Axial T_1 image showing linear, gyriform hyperintensity in the right medial occipital cortex of Patient CP-3A (cortical laminar necrosis).

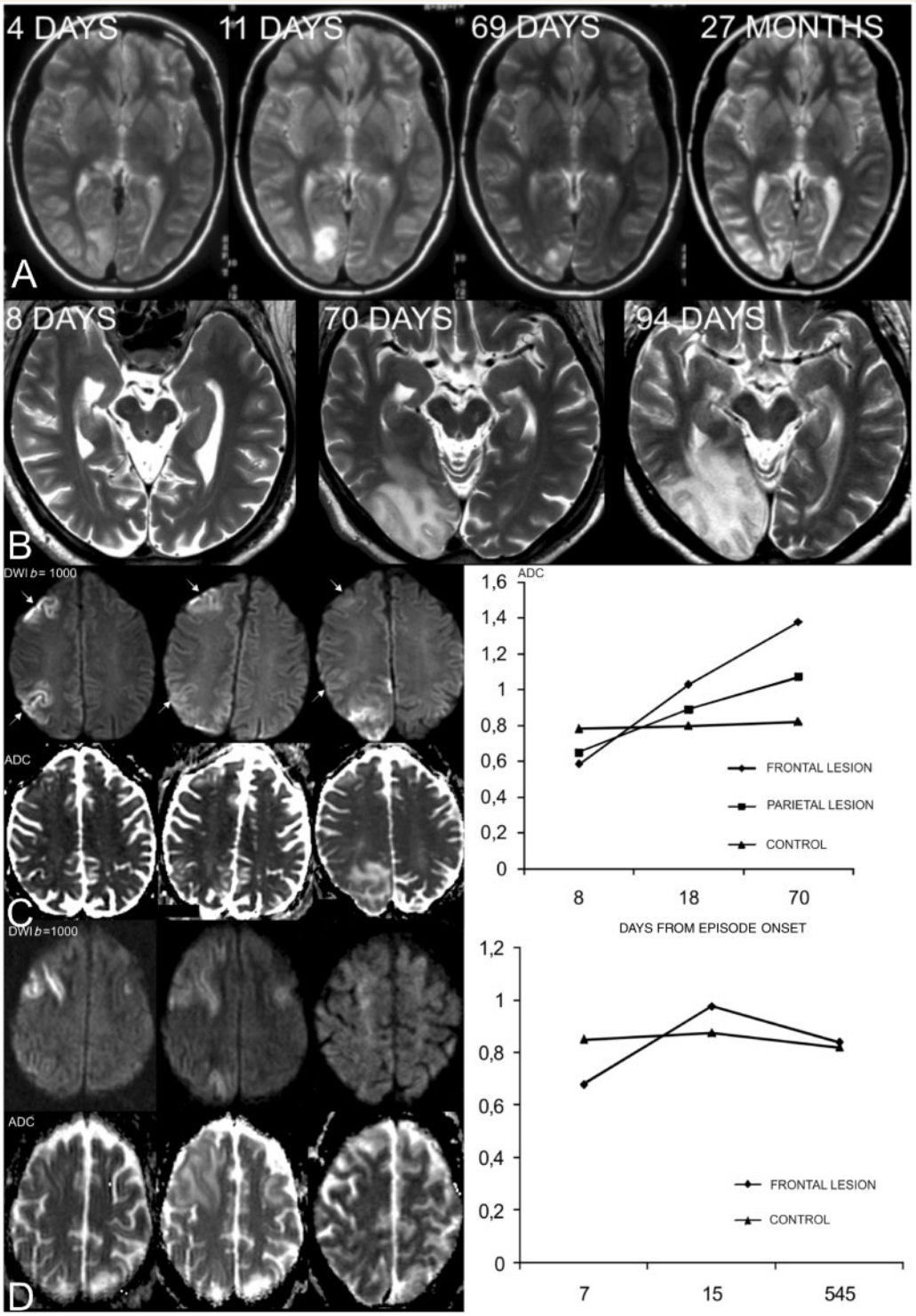

Figure 2 Natural evolution of the stroke-like lesion in POLG-encephalopathy. (**A** and **B**) Axial T_2-weighted images. Times on the images refer to intervals between episode onset and MRI. (**A**) Development, progression and later regression of a medial right occipital lesion in Patient WS-6A. The patient survived the episode. Follow-up imaging 27 months later shows focal atrophy of the occipital area. (**B**) Progression of a large right occipital lesion in Patient AT-1B. The lesion did not regress and the patient did not survive the episode. (**C** and **D**) Diffusion weighted imaging signal and apparent diffusion coefficient (ADC) evolution of cortical lesions during exacerbation episodes. (**C**) Patient AT-1B: images and apparent diffusion coefficient measurements are performed 8, 18 and 70 days after the clinical onset of the episode. Apparent diffusion coefficients are measured in the evolving right frontal and parietal cortical lesions and contralateral uninvolved cortex (control). On Day 70 a right occipital lesion is also seen spreading into the adjacent parietal area. (**D**) Patient AT-2A: images and apparent diffusion coefficient measurements are performed 7, 15 and 545 days after the clinical onset of the episode. Apparent diffusion coefficients are measured in the evolving right frontal cortical lesion and contralateral unaffected cortex. An expanding smaller left frontal lesion is also seen and on Day 15 a right parieto-occipital lesion appears.

Table 1 MRI findings in 32 patients with POLG associated encephalopathy

Patient	Age at onset, years	Age at death, years	Ataxia	Epilepsy	EE	Liver disease	Stroke-like lesions	Thalamus	Inferior olivary nuclei	Cerebellum					Generalized cerebral atrophy
										Cortex	WM	Dentates	Atrophy	Total	
AT-1A	15	44	+	+	+	–	BO, LP, pons	B	–	–	B	–	+	+	–
AT-1B	8	47	+	+	+	–	RPO, LP, BF	–	–	–	B	–	+	+	+
AT-2A	17	53	+	+	+	+	BF, RP	–	–	L	–	–	+	+	–
AT-2B	5	55	+	+	+	–	–	–	–	–	–	–	+	+	+
AT-3A	15	–	+	+	+	–	–	–	–	–	–	–	–	–	–
AT-4A	15	–	+	–	–	–	–	–	–	–	–	–	+	+	–
n = 6			100%	83%	83%	17%	50%	17%	0	17%	33%	0	83%	83%	33%
CP-1A	36	–	+	–	–	–	–	–	–	–	–	T_2 loss	+	+	–
CP-2A	24	–	+	–	–	–	–	–	–	–	–	–	+	+	–
CP-3A	20	20	+	+	+	+	RO	B	–	–	–	T_2 loss	+	+	–
CP-4A	14	23	+	+	+	+	BO, BP, RF	–	–	L	–	?	–	+	–
CP-4B	15	21	+	+	+	+	LTO, RO, BF, RCE	L	–	–	–	?	–	–	–
CP-6A	13	13	+	+	+	+	LO	L	–	–	–	–	–	–	–
n = 6			100%	67%	67%	67%	67%	50%	0	17%	0	33%	50%	67%	0
WS-1A	6	41	+	+	+	–	RO, RF	B	B	–	B	Atrophy	+	+	+
WS-2A	16	24	+	+	+	+	RO	B	–	–	–	–	+	+	–
WS-3A	17	–	+	+	+	–	BO	B	B	–	–	Atrophy	+	+	+
WS-4A	19	–	+	+	+	+	LP	L	B	B	–	Atrophy	+	+	+
WS-5A	12	–	+	–	–	–	–	–	–	B	–	–	+	+	–
WS-6A	17	–	+	+	+	–	RO, RP	B	–	–	–	–	–	–	–
WS-7A	4	30	+	+	+	+	BO, LF, LP, BT	B	–	–	R	–	+	+	+
WS-7B	2	22	+	+	+	+	LO, LP, BF	B	B	–	–	?	+	+	+
WS-8A	12	28	+	+	+	–	BF. BP, LTO	B	–	–	–	T_2 loss	–	+	–
WS-9A	2	13	+	+	+	–	BO, LP	B	B	–	–	T_2 loss	+	+	+
WS-10A	18	–	+	+	+	+	RF, LO,RCE	R	B	–	–	Atrophy	+	+	+
WS-11A	17	–	?	+	+	–	LO	B	–	–	–	–	–	–	–
WS-12A	15	57	+	+	+	–	–	B	–	–	B	?	+	+	–
WS-14A	21	–	+	–	–	–	–	B	B	–	–	T_2 loss	+	+	–
WS-15A	20	–	+	–	–	–	–	B	–	B	–	T_2 loss	+	+	+
WS-18A	45	–	+	–	–	–	–	–	B	B	–	T_2 loss	+	+	+
n = 16	15	31	94%	75%	75%	31%	69%	88%	50%	38%	19%	56%	81%	88%	56%
MSCAE *n* = 28			96%	75%	75%	36%	64%	64%	29%	29%	18%	39%	75%	82%	39%
AL-1A	0.9	1.08	–	+	+	+	BF, RCE	–	–	–	–	–	–	–	–
AL-1B	2	8	+	+	+	–	BTPO	–	–	–	–	–	–	–	–
AL-2A	0.6	0.65	–	+	+	+	LF	–	–	–	–	–	–	–	–
AL-3A	1	1.4	–	+	+	+	BTPO, LCE	–	–	–	–	–	–	–	–
Alpers' *n* = 4			25%	100%	100%	75%	100%	0	0	0	0	0	0	0	0

AT, WS and CP denote the genotype of the patients with MSCAE (AT = A467T homozygous, WS = W748S; CP = A467T/W748S). The Alpers' patients are coded as AL. Numbers symbolize the family and letters the individual. Individuals with the same mutation and number, but different letters are siblings. EE = exacerbation episodes with epilepsy and encephalopathy; F = frontal; P = parietal; T = temporal; O = occipital; R = right; L = left; B = bilateral; CE = cerebellum; WM = white matter; ? = Image quality did not allow for evaluation of dentates.

Clinical improvement of the episodes was associated with regression of the stroke-like lesions, which was replaced by focal atrophy, retraction and often some persisting high T_2 signal (Fig. 2A). The type and degree of residual disability after episode resolution correlated with its localization and was roughly proportional to lesion extent and severity. The commonest form of persisting disability after an episode was cortical visual dysfunction caused by occipital stroke-like lesions and ranging from focal scotomas and haemianopsia to cortical blindness. Central motor sequelae were caused by frontal lesions and a general decline of cognitive functions was associated with the accelerated cerebral atrophy that often ensued after episodes. In two cases, CP-3A and WS-6A, an occipital stroke-like lesion showed late appearing (~60 days from onset of the exacerbation) gyriform, cortical hyperintensity on unenhanced T_1 sequences (Fig. 1G).

Chronic MRI lesions of the thalamus, cerebellum and inferior olivary nuclei were common in MSCAE, but were not seen in Alpers' patients (Fig. 1C–E). Thalamic lesions occurred in 18 out of 28 MSCAE patients, were usually bilateral and showed a predilection for the posterior thalamus including the pulvinar. These lesions developed insidiously and persisted unchanged throughout the disease. Chronic cerebellar MRI abnormalities were seen in 23 out of 28 patients with MSCAE. They comprised atrophy, one or more small cortical/subcortical T_2 hyperintensities (in contrast to

cerebellar stroke-like lesions, these were stable and not associated with clinical episodes), diffuse, symmetrical white matter T_2 hyperintensities and atrophy of the dentate nuclei (Fig. 1A–C). Dentate atrophy was seen in four W748S homozygous patients all of whom also had bilateral lesions of the inferior olives. Loss of the dentate T_2 hypointensity was noted in a further seven patients. No dentate abnormalities where seen in A467T homozygous patients. Cerebellar white matter lesions appeared to be more common in A467T homozygotes (33% versus 19% in the W748S) and were never seen in compound heterozygotes. Bilateral inferior olivary lesions were seen in eight patients, all W748S homozygotes (Fig. 1D), four of whom had atrophy of the dentates. Loss of the dentate signal was seen in another three and could not be excluded in one. Only one patient with bilateral olivary lesions (WS-4A) exhibited palatal tremor/myoclonus.

Cerebral atrophy was found in 11 out of 28 patients with MSCAE and was slowly progressive, mirroring the severity of cognitive impairment, but often accelerated dramatically after exacerbation episodes. Cerebral atrophy was not seen in the Alpers' patients.

Diffusion studies

The most sensitive sequence for detecting fresh stroke-like lesions was heavily weighted diffusion weighted imaging ($b = 1000$). In stroke-like lesions examined in the acute phase (1–8 days from clinical onset), diffusion weighted imaging invariably exhibited high signal. Lesion apparent diffusion coefficient values were low averaging 0.64 (range 0.53–0.79) compared with 0.84 (range 0.73–0.95) in control areas. Subsequently, apparent diffusion coefficient values increased over days to weeks to exceed those of the control areas and later fell. In Patient AT-2A, who survived an exacerbation episode, cortical apparent diffusion coefficient had normalized after 1.5 years (Supplementary Table, Fig. 2C and D). Thalamic and olivary lesions were not identified by diffusion imaging.

Contrast-enhanced MRI and magnetic resonance angiography

Contrast-enhanced MRI was performed in six patients. Minimal cortical lesion enhancement was seen in only two cases (CP-3A, WS-8A in whom it developed late, 50 days after onset of the exacerbation episodes with epilepsy and encephalopathy and 20 days after the discovery of the cortical lesions on MRI. Patient AL-1B showed leptomeningeal, but no parenchymal enhancement. Thalamic, cerebellar and olivary lesions did not enhance. Magnetic resonance angiography was performed in three patients with new cortical lesions and conventional cerebral angiography in one, and showed no abnormalities.

Magnetic resonance spectroscopy

Spectra obtained from fresh cortical lesions showed significantly decreased *N*-acetyl-aspartate and prominent lactate peaks (Fig. 3). Areas with normal MRI signals revealed normal spectra. Interestingly, the old cerebellar white matter lesion in Patient AT-1A also revealed a normal magnetic resonance spectroscopy pattern.

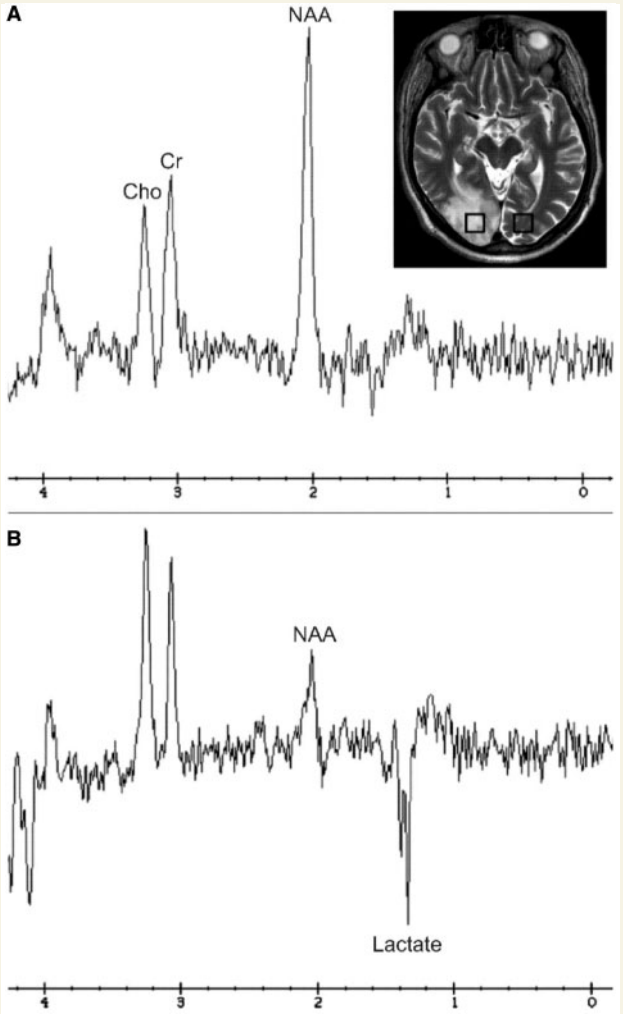

Figure 3 Magnetic resonance spectroscopy of Patient AT-1B. Spectra from the unaffected occipital area (**A**) are normal. Spectra from the right occipital lesion (**B**) show a decrease in *N*-acetyl-aspartate (NAA) and a prominent lactate peak at 1.3 ppm, inverting at 144 ms acquisition time. Cho = choline; Cr = creatine.

Pathology

Cerebral cortical lesions showed severe neuronal loss with vacuolation of the neuropil, astrocytosis and microglial activation. Of the few remaining neurons, some had normal appearance, while most exhibited intense cytoplasmic eosinophilia and pyknotic, dark nuclei (eosinophilic necrosis). Cortical neuronal loss was most severe in superficial and deep cortical layers creating a laminar pattern (Fig. 4A and B). Radiologically uninvolved cortex showed no significant histological changes except in one case (AT-1A) in whom occasional eosinophilic, necrotic neurons with minor vacuolation were seen in the radiologically non-involved, left occipital

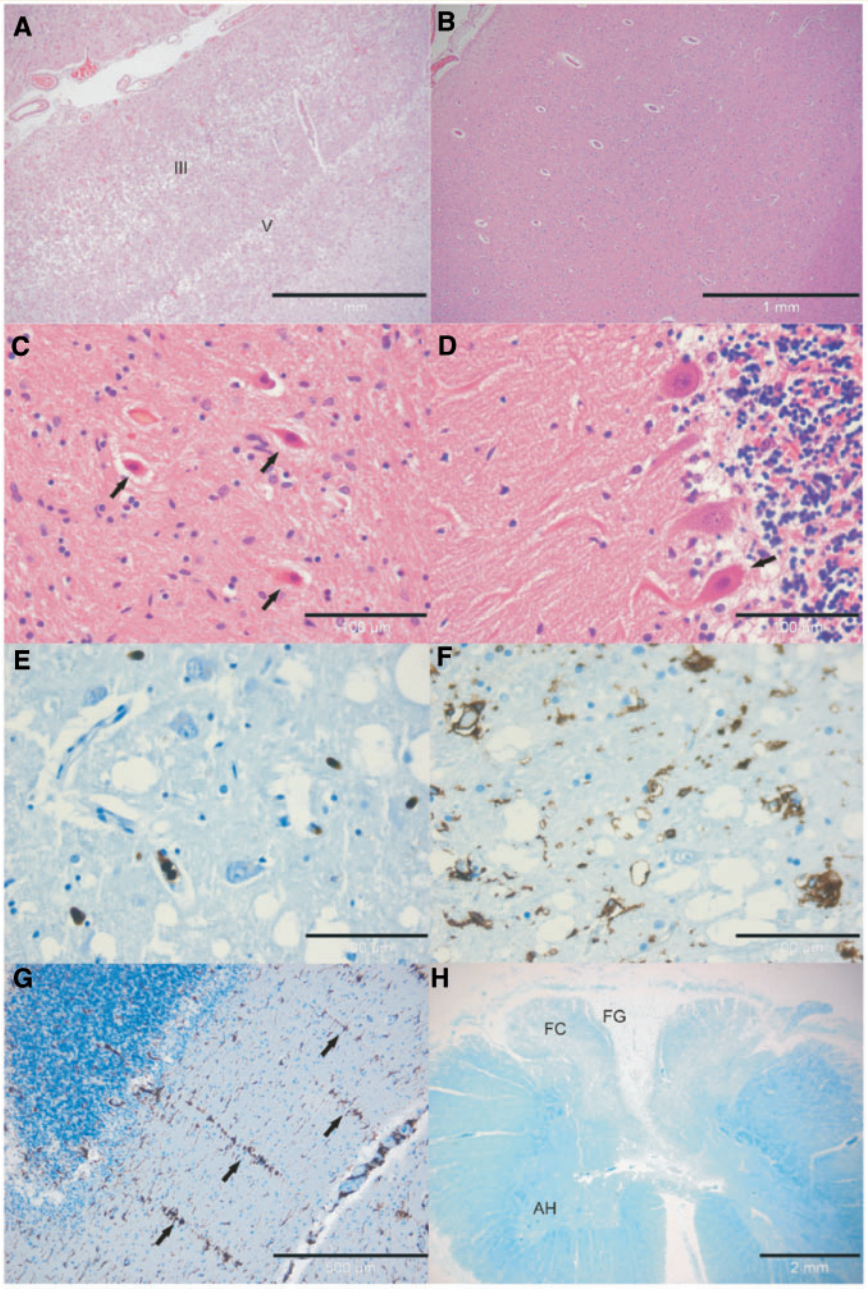

Figure 4 Pathology. (**A–F**) are from Patient AT-1B. Staining; (**A–D**) Haematoxylin-eosin; (**E** and **G**) immunostaining for HLA DR/DP/DQ; (**F**) immunostaining for Mac58; (**H**) luxol fast blue. The size of the bar is given on each microphotograph. (**A**) Laminar cortical lesions affecting predominantly the third and fifth cortical layers of the right occipital lobe. (**B**) The left occipital cortex from the same patient shows no obvious abnormalities. (**C**) Eosinophilic necrosis of dentate neurons (arrows). (**D**) Eosinophilic necrosis of Purkinje cell in the cerebellum (arrow). (**E**) Section from thalamus showing microglial activation and transformation. (**F**) Mac58 immunostaining of the same tissue block as in **E** shows staining only of intravascular monocytes indicating that HLA-DR positive, parenchymatous cells are indeed transformed microglia. (**G**) HLA-DR staining of the cerebellum of Patient WS-1A showing radial microglial activation (arrows) in the molecular layer. (**H**) Luxol fast blue staining of the spinal cord of Patient AT-1A showing selective degeneration of the dorsal column. The fasciculus gracilis (FG) is more severely affected than the fasciculus cuneatus (FC). AH = anterior horn.

cortex. Eosinophilic necrosis and vacuolation also occurred in the thalamus. Here neuronal necrosis seemed more selective than in the cortex, with eosinophilic neurons forming an apparently random mosaic with normal-looking neurons. In Patients AT-1A and AT-1B, histological findings correlated well with the MRI while in WS-1A, MRI showed mild, but definite hyperintensities despite normal thalamic histology. The cerebellum showed selective Purkinje cell loss, eosinophilic necrosis and Bergman's gliosis

(Fig. 4D). The cerebellar white matter showed sponginess and gliosis in Patients AT-1A and AT-1B, who had extensive MRI high signal changes in that area. In the dentate nuclei, there was extensive eosinophilic neuronal necrosis in Patients AT-1A and AT-1B and atrophy in Patient WS-1A (Fig. 4C).

HLA–DR, DP, DQ immunostaining revealed extensive microglial activation in lesions, while monocyte/macrophage immunocytochemistry (anti MAC58) stained almost exclusively intravascular cells (Fig. 4E and F). In the cerebellum of Patient WS-1A, we found extensive microglial proliferation forming radial, linear bands extending from the Purkinje cell layer throughout the molecular layer (Fig. 4G). The basal ganglia, hippocampal structures and pontine nuclei were all unremarkable. The cerebral vasculature was unremarkable both grossly and microscopically. In the spinal cord, there was selective dorsal column degeneration mainly affecting the fasciculus gracilis (Fig. 4H).

Cytochrome oxidase/succinate dehydrogenase histochemistry revealed no cytochrome oxidase deficient or succinate dehydrogenase hyperintense vessels in the cerebrum or cerebellum in either of the patients studied. In AT-1A, we found a few scattered cytochrome oxidase negative/succinate dehydrogenase reactive neurons spread throughout the occipital cortex and, to a lesser extent, the cerebellar cortex.

Discussion

Although POLG-related encephalopathies such as Alpers' and MSCAE vary in genotype, age of onset, clinical picture and severity, our findings suggest that they are parts of the same clinical and pathophysiological continuum. Both share episodic exacerbations with rapidly progressive encephalopathy, epileptic seizures and development of stroke-like lesions with characteristics of neuronal energy failure.

MRI detects abnormalities in the great majority of patients early in the course of the disease and sensitivity increases with disease duration. The combination of thalamic and cortical lesions, in the absence of basal ganglia involvement, is highly suggestive of MSCAE and if deep cerebellar and/or inferior olivary lesions are also present, the picture is, to the best of our knowledge, specific. In Alpers' disease, cortical stroke-like lesions may often be the only finding although thalamic changes occurring early have been described (Wolf *et al*., 2009). While stroke-like lesions may be confused with ischaemic lesions or encephalitis, the lesion predilection for the posterior parts of the cerebrum should prompt POLG genotyping (Wolf *et al*., 2009).

The syndrome of mitochondrial encephalomyopathy lactic acidosis and stroke-like episodes (MELAS) is also commonly associated with stroke-like lesions. In both MELAS (Tzoulis and Bindoff, 2009) and POLG-encephalopathy, acute lesions may show restricted diffusion and cortical histology is similar (Betts *et al*., 2006). There are, however, also important differences. The caudate, lentiform nuclei and dentate nuclei are commonly calcified in MELAS, but not in POLG-encephalopathies. Stroke-like lesion distribution also differs; while occipital involvement is common in both disorders, temporal lesions are very common in MELAS (Iizuka *et al*., 2003) but rare in MSCAE. Furthermore, stroke-like lesions in MELAS often start in the temporal lobes, while in MSCAE these are usually the result of occipital lesion expansion. Histochemistry also appears to differ. Mosaics of cytochrome oxidase negative neurons and skeletal muscle fibres may be seen in both conditions (Winterthun *et al*., 2005; Betts *et al*., 2006). Cytochrome oxidase negative/succinate dehydrogenase reactive vessels, which are typically present in striated muscle and brain of patients with MELAS, have not been described in muscle of patients with POLG-associated disease (Rantamäki *et al*., 2001; Van Goethem *et al*., 2004; Winterthun *et al*., 2005) and were not found in the brain of two of our patients.

The stroke-like lesions of POLG encephalopathies evolve dynamically and mirror the clinical course. The localization, extent and progression of stroke-like lesions have important prognostic implications and our data suggest that it is important to monitor lesion evolution. Gradual regression or disappearance of the lesions strongly suggests potential for recovery and may influence clinical decision taking on further treatment.

Stroke-like lesions show restricted water diffusion in the acute phase suggesting intracellular water sequestration i.e. cytotoxic cerebral oedema. Histopathological examination shows that neurons are selectively lost in these lesions. In the absence of signs of angiopathy and ischaemia, the most likely explanation for this phenomenon is neuronal ATP deficiency caused by failure of the mitochondrial respiratory chain to meet the high energy demand. Epilepsy will significantly aggravate, and may even trigger stroke-like lesions, either by increasing neuronal energy consumption or via direct excitotoxic effects. While incomplete, our data show that epileptic activity may be absent early in the course of an exacerbation episode and that progression can still occur even when previously documented epileptic activity disappears. Ongoing epileptic activity is not, therefore, a prerequisite for stroke-like lesion expansion or clinical progression. Currently there are insufficient data, but it appears unlikely that epileptic activity is the primary mechanism behind the exacerbation episodes and stroke-like lesions in POLG-encephalopathy.

Further support for energy depletion comes from the finding of cortical laminar necrosis. Cortical laminar necrosis is believed to represent selective damage of the cortical layers that are most sensitive to ATP deficiency; the subsequent intracortical microhaemorrhage or infiltration by fat-laden macrophages accounts for the shortening of T_1 signal (Takahashi *et al*., 1993). Neuronal energy deficiency is also supported by the histological findings of selective neuronal loss and eosinophilic necrosis in the cerebral cortex and thalamus, selective loss of Purkinje cells and dentate neurons in the cerebellum, laminar cortical necrosis and neuronal cytochrome oxidase-deficiency. Similar histological findings, restricted water diffusion and cortical laminar necrosis have been associated with states of secondary CNS energy deficiency such as cerebral ischaemia/hypoxia (Takahashi *et al*., 1993; Schaefer *et al.,* 2000; Siskas *et al*., 2003; Mena *et al*., 2004), carbon monoxide poisoning (Uemura *et al*., 2001, Kondo *et al*., 2007; Lo *et al*., 2007), cyanide poisoning (Rachinger *et al* 2002; Riudavets *et al*., 2005) and hypoglycaemic encephalopathy (Fujioka *et al*., 1997; Böttcher *et al*., 2005; Yoneda *et al*., 2005).

Chronic MRI lesions and histopathological changes affecting the thalamus, cerebellum and brainstem in MSCAE have been reported earlier (Rantamäki *et al*., 2001; Van Goethem *et al*., 2004). Thalamic lesions are very typical of MSCAE. The suggestion that these arise secondarily to status epilepticus (Szabo *et al*., 2005) is not supported by our studies. Seven patients with epilepsy lacked MRI evidence of thalamic involvement while two without epilepsy (WS-14A, WS-15A) had bilateral, prominent thalamic changes. Apparently, mitochondrial dysfunction alone is capable of producing these lesions. Cerebellar cortical and dentate involvement is consistent with cerebellofugal degeneration, while white matter involvement may represent general loss of the cerebellar connections. Similar MRI and histological findings in the cerebellum have been reported in patients with Kearns–Sayre syndrome (Chu *et al*., 1999; Tanji *et al*., 1999). Moreover, synaptic immunohistochemistry studies in Kearns–Sayre syndrome have shown evidence of Purkinje cell disconnection at the dentate nucleus, i.e. loss of cerebellar efferents (Tanji *et al*., 1999). Radial microglial proliferation in the molecular layer of the cerebellar cortex (Fig. 4G) has been described in models of drug toxicity and cerebral contusion injury and is thought to represent microglial activation along the dentritic processes of injured Purkinje cells (Näkki *et al*., 1995; O'Hearn *et al*., 1997; Igarashi *et al*., 2007).

Olivary lesions are suggestive of hypertrophic olivary degeneration, which usually occurs secondarily to de-afferentation of the inferior olives by lesions interrupting the Guillain–Mollaret triangle (Yokota *et al*., 1989). Evidence of bilateral dentate atrophy was found in four out of eight patients with olivary changes and dentate involvement could not be excluded in the remaining four. Classically, this type of olivary lesion has been associated with palatal tremor/myoclonus, but this was only seen in one case (Tzoulis *et al*., 2006; Johansen *et al*., 2008). Interestingly, olivary lesions only occurred in W748S homozygotes, but the reason for this remains unclear. Selective degeneration of the dorsal columns, particularly the fasciculus gracilis that carries sensory input from the lower limbs, correlates well with the clinical findings of a sensory gait ataxia.

Our findings suggest that energy failure is a major factor in the pathogenesis of POLG-encephalopathies. By generating cortical injury, it predisposes to epileptogenesis, which in turn potentiates neuronal damage by increasing the energy demands of already compromised cells. This results in a self-perpetuating cycle. What explains the characteristic predilection for occipital and other neocortical areas, thalamus and cerebellum is unclear. High energy requirement alone is unlikely to be the sole cause since the hippocampus and striatum, which are known to be highly sensitive to energy depletion due to other causes, are consistently spared as are the central motor neurons. This implies that the pathogenesis of POLG-associated disease involves other factors and further studies at the molecular level are required to clarify the complex pathomechanism of this disorder.

Acknowledgements

The expert technical assistance of Mrs Laila Vårdal and Mrs Edith Fick is gratefully acknowledged.

Funding

Helse Vest (CT, LAB); The Norwegian Research council (LAB): Pierfranco and Luisa Mariani Foundation; Telethon-Italy Foundation grant n°GGP07019; the Italian Ministry of Health grant RF-INN-2007-634163 (MZ).

Supplementary material

Supplementary material is available at *Brain* online.

References

Betts J, Jaros E, Perry RH, Schaefer AM, Taylor RW, Abdel-All Z, et al. Molecular neuropathology of MELAS: level of heteroplasmy in individual neurones and evidence of extensive vascular involvement. Neuropathol Appl Neurobiol 2006; 32: 359–73.

Böttcher J, Kunze A, Kurrat C, Schmidt P, Hagemann G, Witte OW, et al. Localized reversible reduction of apparent diffusion coefficient in transient hypoglycemia-induced hemiparesis. Stroke 2005; 36: e20–2.

Chu BC, Terae S, Takahashi C, Kikuchi Y, Miyasaka K, Abe S, et al. MRI of the brain in the Kearns-Sayre syndrome: report of four cases and a review. Neuroradiology 1999; 41: 759–64.

Del Bo R, Bordoni A, Sciacco M, Di Fonzo A, Galbiati S, Crimi M, et al. Remarkable infidelity of polymerase gamma A associated with mutations in POLG1 exonuclease domain. Neurology 2003; 61: 903–8.

de Vries MC, Rodenburg RJ, Morava E, van Kaauwen EP, ter Laak H, Mullaart RA, et al. Multiple oxidative phosphorylation deficiencies in severe childhood multi-system disorders due to polymerase gamma (POLG1) mutations. Eur J Pediatr 2007; 166: 229–34.

Engelsen BA, Tzoulis C, Karlsen B, Lillebø A, Laegreid LM, Aasly J, et al. POLG1 mutations cause a syndromic epilepsy with occipital lobe predilection. Brain 2008; 131: 818–28.

Ferrari G, Lamantea E, Donati A, Filosto M, Briem E, Carrara F, et al. Infantile hepatocerebral syndromes associated with mutations in the mitochondrial DNA polymerase-gammaA. Brain 2005; 128: 723–31.

Fujioka M, Okuchi K, Hiramatsu KI, Sakaki T, Sakaguchi S, Ishii Y. Specific changes in human brain after hypoglycemic injury. Stroke 1997; 28: 584–7.

Hakonen AH, Goffart S, Marjavaara S, Paetau A, Cooper H, Mattila K, et al. Infantile-onset spinocerebellar ataxia and mitochondrial recessive ataxia syndrome are associated with neuronal complex I defect and mtDNA depletion. Hum Mol Genet 2008; 17: 3822–35.

Hakonen AH, Heiskanen S, Juvonen V, Lappalainen I, Luoma PT, Rantamaki M, et al. Mitochondrial DNA polymerase W748S mutation: a common cause of autosomal recessive ataxia with ancient European origin. Am J Hum Genet 2005; 77: 430–41.

Igarashi T, Potts MB, Noble-Haeusslein LJ. Injury severity determines Purkinje cell loss and microglial activation in the cerebellum after cortical contusion injury. Exp Neurol 2007; 203: 258–68.

Iizuka T, Sakai F, Kan S, Suzuki N. Slowly progressive spread of the stroke-like lesions in MELAS. Neurology 2003; 61: 1238–44.

Johansen KK, Bindoff LA, Rydland J, Aasly JO. Palatal tremor and facial dyskinesia in a patient with POLG1 mutation. Mov Disord 2008; 23: 1624–6.

Kondo A, Saito Y, Seki A, Sugiura C, Maegaki Y, Nakayama Y, et al. Delayed neuropsychiatric syndrome in a child following carbon monoxide poisoning. Brain Dev 2007; 29: 174–7.

Lo CP, Chen SY, Lee KW, Chen WL, Chen CY, Hsueh CJ, et al. Brain injury after acute carbon monoxide poisoning: early and late complications. AJR Am J Roentgenol 2007; 189: W205–11.

Mena H, Cadavid D, Rushing EJ. Human cerebral infarct: a proposed histopathologic classification based on 137 cases. Acta Neuropathol 2004; 108: 524–30.

Nguyen KV, Østergaard E, Ravn SH, Balslev T, Danielsen ER, Vardag A, et al. POLG mutations in Alpers syndrome. Neurology 2005; 65: 1493–5.

Näkki R, Koistinaho J, Sharp FR, Sagar SM. Cerebellar toxicity of phencyclidine. J Neurosci 1995; 15: 2097–108.

O'Hearn E, Molliver ME. The olivocerebellar projection mediates ibogaine-induced degeneration of Purkinje cells: a model of indirect, trans-synaptic excitotoxicity. J Neurosci 1997; 17: 8828–41.

Rachinger J, Fellner FA, Stieglbauer K, Trenkler J. MR changes after acute cyanide intoxication. AJNR Am J Neuroradiol 2002; 23: 1398–401.

Rantamäki M, Krahe R, Paetau A, Cormand B, Mononen I, Udd B. Adult-onset autosomal recessive ataxia with thalamic lesions in a Finnish family. Neurology 2001; 57: 1043–9.

Riudavets MA, Aronica-Pollak P, Troncoso JC. Pseudolaminar necrosis in cyanide intoxication: a neuropathology case report. Am J Forensic Med Pathol 2005; 26: 189–91.

Sarzi E, Bourdon A, Chrétien D, Zarhrate M, Corcos J, Slama A, et al. Mitochondrial DNA depletion is a prevalent cause of multiple respiratory chain deficiency in childhood. J Pediatr 2007 M; 150: 531–4, 534.e1–6.

Schaefer PW, Grant PE, Gonzalez RG. Diffusion-weighted MR imaging of the brain. Radiology 2000; 217: 331–45.

Siskas N, Lefkopoulos A, Ioannidis I, Charitandi A, Dimitriadis AS. Cortical laminar necrosis in brain infarcts: serial MRI. Neuroradiology 2003; 45: 283–8.

Szabo K, Poepel A, Pohlmann-Eden B, Hirsch J, Back T, Sedlaczek O, et al. Diffusion-weighted and perfusion MRI demonstrates parenchymal changes in complex partial status epilepticus. Brain 2005; 128: 1369–76.

Takahashi S, Higano S, Ishii K, Matsumoto K, Sakamoto K, Iwasaki Y, et al. Hypoxic brain damage: cortical laminar necrosis and delayed changes in white matter at sequential MR imaging. Radiology 1993; 189: 449–56.

Tanji K, DiMauro S, Bonilla E. Disconnection of cerebellar Purkinje cells in Kearns-Sayre syndrome. J Neurol Sci 1999; 166: 64–70.

Tzoulis C, Bindoff LA. Serial diffusion imaging in a case of mitochondrial encephalomyopathy, lactic acidosis, and stroke-like episodes. Stroke 2009; 40: e15–7.

Tzoulis C, Engelsen BA, Telstad W, Aasly J, Zeviani M, Winterthun S, et al. The spectrum of clinical disease caused by the A467T and W748S POLG mutations: a study of 26 cases. Brain 2006; 129: 1685–92.

Uemura K, Harada K, Sadamitsu D, Tsuruta R, Takahashi M, Aki T, et al. Apoptotic and necrotic brain lesions in a fatal case of carbon monoxide poisoning. Forensic Sci Int 2001; 116: 213–9.

Van Goethem G, Luoma P, Rantamäki M, Al Memar A, Kaakkola S, Hackman P, et al. POLG mutations in neurodegenerative disorders with ataxia but no muscle involvement. Neurology 2004; 63: 1251–7.

Winterthun S, Ferrari G, He L, Taylor RW, Zeviani M, Turnbull DM, et al. Autosomal recessive mitochondrial ataxic syndrome due to mitochondrial polymerase gamma mutations. Neurology 2005; 64: 1204–8.

Wolf NI, Rahman S, Schmitt B, Taanman JW, Duncan AJ, Harting I, et al. Status epilepticus in children with Alpers' disease caused by POLG1 mutations: EEG and MRI features. Epilepsia 2009; 50: 1596–607.

Yokota T, Hirashima F, Furukawa T, Tsukagoshi H, Yoshikawa H. MRI findings of inferior olives in palatal myoclonus. J Neurol 1989; 236: 115–6.

Yoneda Y, Yamamoto S. Cerebral cortical laminar necrosis on diffusion-weighted MRI in hypoglycaemic encephalopathy. Diabet Med 2005; 22: 1098–100.